

Reconstituted Slow Muscarinic Inhibition of Neuronal (Ca_v1.2c) L-Type Ca²⁺ Channels

Roger A. Bannister,* Karim Melliti,[†] and Brett A. Adams*

*Department of Biology, Utah State University, Logan, Utah 84322 USA; and [†]Merck, Sharp, and Dohme Research Laboratories, The Neuroscience Research Center, Terlings Park, Harlow, Essex CM20 2QR, United Kingdom

ABSTRACT Ca²⁺ influx through L-type channels is critical for numerous physiological functions. Relatively little is known about modulation of neuronal L-type Ca²⁺ channels. We studied modulation of neuronal Ca_v1.2c channels heterologously expressed in HEK293 cells with each of the known muscarinic acetylcholine receptor subtypes. Gαq/11-coupled M1, M3, and M5 receptors each produced robust inhibition of Ca_v1.2c, whereas Gαi/o-coupled M2 and M4 receptors were ineffective. Channel inhibition through M1 receptors was studied in detail and was found to be kinetically slow, voltage-independent, and pertussis toxin-insensitive. Slow inhibition of Ca_v1.2c was blocked by coexpressing RGS2 or RGS3T or by intracellular dialysis with antibodies directed against Gαq/11. In contrast, inhibition was not reduced by coexpressing βARK1ct or Gαt. These results indicate that slow inhibition required signaling by Gαq/11, but not Gβγ, subunits. Slow inhibition did not require Ca²⁺ transients or Ca²⁺ influx through Ca_v1.2c channels. Additionally, slow inhibition was insensitive to pharmacological inhibitors of phospholipases, protein kinases, and protein phosphatases. Intracellular BAPTA prevented slow inhibition via a mechanism other than Ca²⁺ chelation. The cardiac splice-variant of Ca_v1.2 (Ca_v1.2a) and a splice-variant of the neuronal/neuroendocrine Ca_v1.3 channel also appeared to undergo slow muscarinic inhibition. Thus, slow muscarinic inhibition may be a general characteristic of L-type channels having widespread physiological significance.

INTRODUCTION

Neuronal L-type Ca²⁺ channels perform critical functions in gene expression, neurosecretion, synaptic plasticity, and circadian rhythms (Murphy et al., 1991; Bading et al., 1993; Jensen et al., 1999; Weisskopf et al., 1999; Pennartz et al., 2002). In comparison with N-type and P/Q-type Ca²⁺ channels, little is known about the mechanisms by which neuronal L-type channels are modulated (Dolphin, 1999). Because native cells may express more than one L-type Ca²⁺ channel isoform (Snutch et al., 1991; Forti and Pietrobon, 1993; Hell et al., 1993) and because these different isoforms cannot be easily distinguished using pharmacological tools, the precise molecular identity of endogenous L-type channels is often uncertain. Furthermore, distinct splice-variants of Ca²⁺ channels may be differentially modulated (Page et al., 1998; Shistik et al., 1998; Bourinet et al., 1999; Melliti et al., 2000). For these reasons, expression of L-type channels in heterologous systems can provide information difficult to obtain from native cells.

Five distinct subtypes (M1–M5) of muscarinic acetylcholine receptor are expressed in mammalian brain (Wei et al., 1994). M1, M3, and M5 subtypes couple preferentially to pertussis toxin (PTX)-insensitive Gαq/11 proteins, whereas M2 and M4 receptor subtypes couple mainly to PTX-sensitive Gαi/o proteins (Felder, 1995).

Muscarinic inhibition of native L-type channels has been studied in mammalian central and peripheral neurons (Mathie et al., 1992; Howe and Surmeier, 1995; Stewart et al., 1999). In superior cervical ganglion (SCG) neurons from mice and rats, native L-type channels are inhibited through a slowly activating pathway linked to M1 muscarinic acetylcholine receptors (Bernheim et al., 1992; Shapiro et al., 1999). However, less is known about L-type channel modulation in other cell types (Dolphin, 1999), and the ability of muscarinic receptor subtypes other than M1 to regulate L-type channels has been little explored.

In the present study we reconstituted slow muscarinic inhibition of cloned L-type Ca²⁺ channels transiently expressed in human embryonic kidney (HEK293) cells. We show that all three Gαq/11-coupled muscarinic receptor subtypes (M1, M3, and M5) generate robust inhibition of the neuronal splice-variant Ca_v1.2c. Inhibition of Ca_v1.2c was characterized in detail for M1 receptors and was found to be kinetically slow, voltage-independent, and PTX-insensitive. Slow muscarinic inhibition of Ca_v1.2c was blocked by expression of RGS2 or RGS3T, two regulators of G protein signaling known to interact with Gαq/11. Pharmacological experiments suggest that the underlying signaling pathway does not involve phospholipase A₂, phospholipase C, tyrosine kinases, serine/threonine kinases, or phosphatases. Significantly, we find that the cardiac splice-variant of Ca_v1.2 (Ca_v1.2a) and a splice-variant of the neuronal/neuroendocrine Ca_v1.3 channel also appear to undergo slow muscarinic inhibition. Thus, slow muscarinic inhibition may be a general feature of L-type channels that can influence Ca²⁺ influx in more cell types than previously thought.

Submitted April 29, 2002, and accepted for publication July 24, 2002.

Address reprint requests to Brett A. Adams, Department of Biology, Utah State University, 5305 Old Main Hill, Logan, UT 84322. Tel.: 435-797-7107; Fax: 435-797-1575; E-mail: brett@biology.usu.edu.

© 2002 by the Biophysical Society

0006-3495/02/12/3256/12 \$2.00

MATERIALS AND METHODS

Cell culture and transfection

Human embryonic kidney (HEK293) cells were obtained from the American Type Culture Collection (Manassas, VA) and propagated in culture medium containing 90% DMEM (cat. no. 11995; Invitrogen/Gibco, Rockville, MD), 10% defined fetal bovine serum (Hyclone Labs, Logan, UT), and $50 \mu\text{g ml}^{-1}$ gentamicin. HEK293 cells of low passage number (<20) were trypsinized weekly and replated onto 60 mm culture dishes at $\sim 20\%$ confluence. CaPO_4 precipitation was used to transfect these cells within 3–5 days of plating. The transfection mixture contained expression plasmids encoding a single type of Ca^{2+} channel $\alpha 1$ subunit ($\text{Ca}_v1.2\text{c}$ (Snutch et al., 1991), $\text{Ca}_v1.2\text{a}$ (Mikami et al., 1989), or $\text{Ca}_v1.3$ (Xu and Lipscombe, 2001)). In the case of $\text{Ca}_v1.2\text{c}$ and $\text{Ca}_v1.3$, ancillary $\alpha 2\text{b}$ (rat brain) and $\beta 3$ (rabbit brain) Ca^{2+} channel subunits were cotransfected at $1.25 \mu\text{g}$ of each cDNA per dish. In the case of $\text{Ca}_v1.2\text{a}$, ancillary $\alpha 2\text{a}$ (rabbit skeletal muscle) and $\beta 2\text{a}$ (rabbit heart) Ca^{2+} channel subunits were cotransfected at $1.25 \mu\text{g}$ of each cDNA per dish. An expression plasmid encoding the M1 muscarinic acetylcholine receptor was cotransfected at $0.5 \mu\text{g}$ per dish. In some experiments the M1 receptor was replaced by the M2 receptor ($0.025 \mu\text{g}$ per dish), the M3 receptor (0.125 – $0.625 \mu\text{g}$ per dish), the M4 receptor ($0.125 \mu\text{g}$ per dish), or the M5 receptor ($0.5 \mu\text{g}$ per dish). In selected experiments, the transfection mixture included plasmids encoding $\text{Gly}^{495}\text{-Leu}^{689}$ of β -adrenergic receptor kinase 1 (βARK1ct), rod transducin ($\text{G}\alpha\text{t}$), untagged RGS2 or RGS2 fused in-frame to the carboxyl terminus of enhanced green fluorescent protein (EGFP-RGS2), or EGFP-RGS3T at $1.25 \mu\text{g}$ per dish. Transfections that did not include EGFP-RGS2 or EGFP-RGS3T included a plasmid encoding EGFP at $0.125 \mu\text{g}$ per dish. The day after transfection, cells were briefly trypsinized and replated onto 12 mm round glass coverslips. After replating, cells were incubated at 37°C for 6 h and then held at a lower temperature (29°C) overnight; this last step appeared to promote channel expression. Electrophysiological experiments were performed 24–32 h after replating. Successfully transfected cells were visually identified by their green fluorescence under ultraviolet illumination; only fluorescent cells were used for experiments.

Expression plasmids

cDNAs encoding rat brain $\text{Ca}_v1.2\text{c}$ (GenBank accession number M67515) and rat brain $\alpha 2\text{b}$ (M86621) were in the expression vector pMT2 (Genetics Institute, Cambridge, MA). Rabbit heart $\text{Ca}_v1.2\text{a}$ (X15539) and rabbit skeletal muscle $\alpha 2\text{a}$ (M21948) were in pKCRH2 (Mishina et al., 1984). Rat superior cervical ganglion neuron $\text{Ca}_v1.3$ (splice variant +11/ $\Delta 32/42\text{a}$; AF370009) was in pcDNA6/V5-HisB (Invitrogen, Carlsbad, CA). Rabbit brain $\beta 3$ (X64300) was in pcDNA3 (Invitrogen). Rabbit heart $\beta 2\text{a}$ (X64297) was in pcDNA3.1+ (Invitrogen). Human M1 muscarinic acetylcholine receptor (X52068) was in pCD (Okayama and Berg, 1983). Jellyfish enhanced green fluorescent protein (U55763) was in pEGFP (Clontech, Cambridge, UK). Human M2 muscarinic acetylcholine receptor (X15264) and bovine βARK1ct (M34019) were in pRK5 (Koch et al., 1994). Human $\text{G}\alpha\text{t}$ (X63749), human M3 muscarinic acetylcholine receptor (X15266), human M4 muscarinic acetylcholine receptor (X15265), and human M5 muscarinic acetylcholine receptor (M80333) were in pcDNA 3.1+. Human RGS2 (L13463) was in pcDNA3.1+ or pEGFP-C2 (Clontech). Human RGS3T (U27655) was in pEGFP-C3 (Clontech).

Electrophysiology

Large-bore patch pipettes were pulled from $100 \mu\text{l}$ borosilicate glass micropipettes and, unless noted otherwise, filled with the standard pipette solution containing (in mM): 155 CsCl, 10 Cs_2EGTA , 4 MgATP, 0.32 LiGTP, and 10 HEPES, adjusted to pH 7.4 with CsOH. In selected experiments, a lower concentration of Cs_2EGTA (0.1 mM) was used, or

Cs_2EGTA was replaced by Cs_4BAPTA (20 mM) and CsCl was reduced accordingly. As a control for BAPTA, we used a pipette solution containing 5,5'-dinitro-BAPTA (20 mM) and 145 CsCl, 10 Cs_2EGTA , 4 MgATP, 0.32 LiGTP and 10 HEPES, pH 7.4 with CsOH. Aliquots of the pipette solutions were stored at -80°C , kept on ice after thawing, and filtered at $0.22 \mu\text{m}$ immediately before use, except where noted. Anti-Gaq/11 or preimmune rabbit IgG were added to the prefiltered standard pipette solution at the indicated concentrations. In one series of experiments, AMP-PNP (5 mM) was substituted for MgATP in the standard pipette solution. On the same day as their use, U-73122 and U-73343 were dissolved in DMSO to make a 10 mM stock solution which was subsequently diluted (1:1000) into prefiltered standard pipette solution. Quinacrine was dissolved in double-distilled water to make a stock of 10 mM (pH adjusted to 7.4 with CsOH) and then diluted (1:100) into prefiltered standard pipette solution. Calcineurin auto-inhibitory peptide (CAIN) was dissolved in prefiltered standard pipette solution. Pipette solutions were not filtered following the addition of anti-Gaq/11, control IgG, U-73122, U-73343, quinacrine, or CAIN. The bath solution contained 145 NaCl, 40 CaCl_2 , 2 KCl, and 10 HEPES, adjusted to pH 7.4 with NaOH. Staurosporine, genistein, and okadaic acid were dissolved in DMSO to make stock solutions of 1 mM, 100 mM, and $100 \mu\text{M}$, respectively; these stocks were stored in the dark at -20°C and diluted into the bath solution immediately before use. The final concentration of DMSO in the bath was 0.01–0.1%, which alone had no effects on Ca^{2+} currents or their modulation. Carbachol (CCh) and atropine were dissolved directly in the bath solution. Application of CCh was by bath exchange or local superfusion through a macropipette positioned close to the cell. Coverslips were discarded following a single exposure to CCh.

Pipette tips were coated with paraffin to reduce capacitance. Filled pipettes had DC resistances of 1.0–1.5 M Ω . Ca^{2+} currents were recorded in the whole-cell, ruptured-patch mode. After forming a gigaohm seal in the cell-attached configuration, residual pipette capacitance was compensated using the negative capacitance circuit of the amplifier. The DC resistance of the whole-cell configuration routinely exceeded 1 G Ω . The steady holding potential was -90 mV . No corrections were made for liquid junction potentials. Ca^{2+} currents were evoked by 10 ms voltage-clamp steps to $+30 \text{ mV}$ (near the peak of the current-voltage relationship; see Fig. 1 b), delivered at 0.2 Hz unless otherwise noted. All Ca^{2+} currents were corrected online for linear cell capacitance and leakage currents using a $-P/4$ subtraction protocol. Leak-subtracted current amplitudes were measured at the time of peak inward current. Currents were filtered at 2–10 kHz using the built-in Bessel filter (four-pole low-pass) of an Axopatch 200B amplifier and sampled at 10–50 kHz using a Digidata 1200 analog-to-digital board installed in a Gateway Pentium computer. The pCLAMP 8.0 software programs Clampex and Clampfit were used for data acquisition and analysis, respectively. Figures were made using the software program Origin (version 6.0).

Linear cell capacitance (C) was determined by integrating the area under the whole-cell capacity transient, which was evoked by a 10 ms voltage-clamp step from -90 to -80 mV . The average value of C was $30 \pm 1 \text{ pF}$ (mean \pm SEM; $n = 237$ cells). Voltage errors were minimized by using low-resistance pipettes and electronic compensation. For each cell, the time constant for decay of the whole-cell capacity transient (τ) was reduced as much as possible using the analog series resistance compensation circuit of the amplifier. Series resistance (R_s) was calculated for each cell as $\tau \times (1/C)$. The average values of τ and R_s , measured before electronic compensation, were $135 \pm 7 \mu\text{s}$ and $4.6 \pm 0.2 \text{ M}\Omega$, respectively. After electronic compensation, the average values of τ and R_s were $98 \pm 5 \mu\text{s}$ and $3.6 \pm 0.1 \text{ M}\Omega$, respectively. Maximal Ca^{2+} current amplitude (test potential $+30 \text{ mV}$) was $1020 \pm 73 \text{ pA}$. Maximal current density was $37 \pm 2 \text{ pA/pF}$. The average maximum voltage error after compensation was $3.1 \pm 0.2 \text{ mV}$. Statistical comparisons were by ANOVA or unpaired two-tailed t -test, with $p < 0.05$ considered significant. Experiments were conducted at room temperature (20 – 24°C).

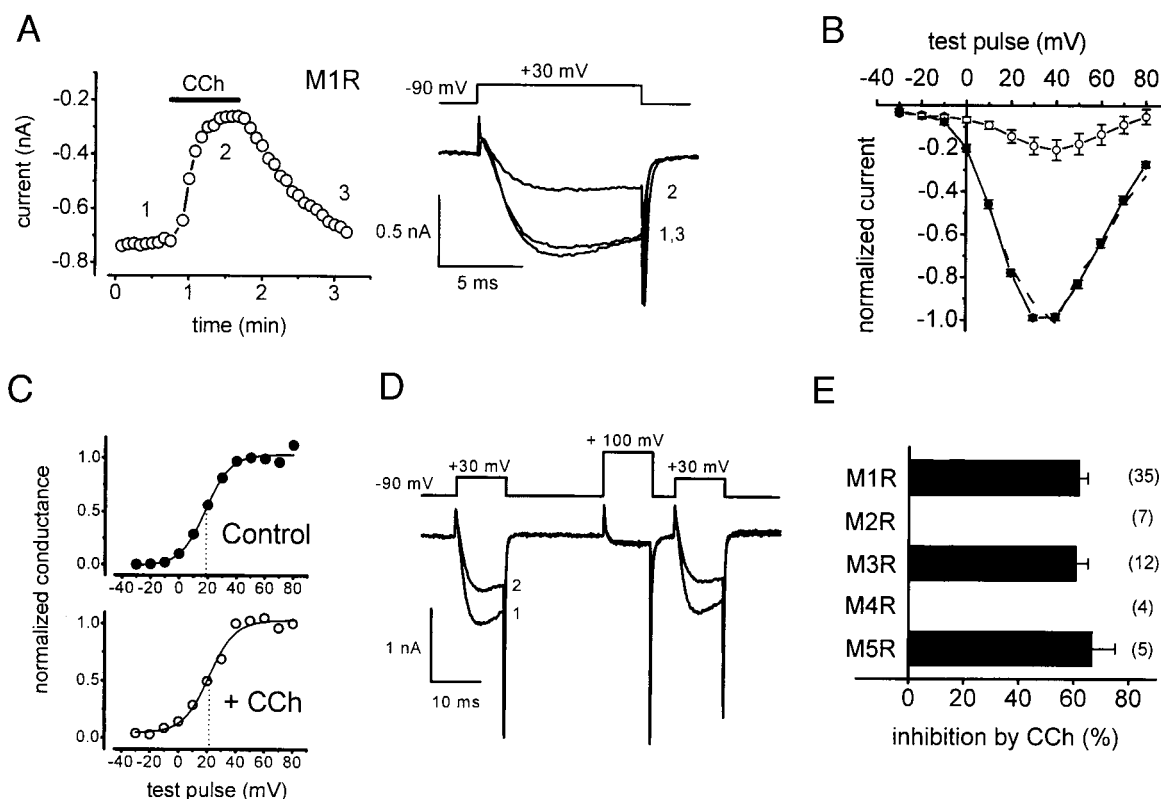


FIGURE 1 Reconstituted slow muscarinic inhibition of neuronal L-type Ca^{2+} channels. Data from cells coexpressing M1 receptors (except in panel *e*) and $\text{Ca}_v1.2c$, $\alpha 2\delta b$, and $\beta 3$ Ca^{2+} channel subunits. The standard pipette solution containing 10 mM EGTA was used. Throughout the figures, application of CCh (1 mM) is indicated by a heavy horizontal line. (*a, left panel*) Time-plot of inhibition through M1 receptors. Ca^{2+} currents were evoked at 0.2 Hz by 10-ms depolarizations from -90 to $+30$ mV. Maximum current amplitudes are plotted versus time. Linear cell capacitance (C) = 17 pF; compensated series resistance (R_s) = 6.1 M Ω ; the maximal voltage error (VE) in this recording was 4.5 mV. (*a, right panel*) Ca^{2+} currents recorded at times indicated in the plot at left. (*b*) Control I - V data (●) were obtained (at 0.2 Hz) before CCh application. CCh was then applied, and the onset of slow inhibition was monitored by depolarizations to $+30$ mV delivered at 0.2 Hz. During steady-state slow inhibition, I - V data (○) were again obtained at 0.2 Hz. Symbols represent data obtained from the same seven cells before and during CCh application. For each cell, current amplitudes were normalized to the peak current recorded before applying CCh. The dashed line is the scaled, inhibited I - V relationship. (*c*) Whole-cell Ca^{2+} conductances were calculated (assuming a reversal potential of $+90$ mV) from I - V data obtained from each cell (e.g., panel *b*) before and during CCh application. The derived conductance data were fit by a Boltzmann function (Origin, version 6.0). The dashed vertical line indicates $V_{1/2}$, the midpoint of activation. (*d*) A standard three-pulse voltage protocol was used to elicit currents before CCh application (1) and during (2) maximal slow inhibition of the Ca^{2+} current. C = 19 pF; R_s = 2.4 M Ω ; VE = 3.0 mV. (*e*) Inhibition of $\text{Ca}_v1.2c$ currents through each of the five muscarinic acetylcholine receptor subtypes. Receptors were activated by 1 mM CCh. Inhibition was measured as $[1 - (\text{inhibited current}/\text{control current})] \times 100\%$. Error bars represent \pm SEM.

Reagents

Preimmune IgG and affinity-purified polyclonal antibody directed against 19 amino acids within the extreme carboxyl termini of $G\alpha q/11$ (sc-392) were purchased from Santa Cruz Biotechnology (Santa Cruz, CA). These preparations were supplied in sterile saline without preservatives. Carbachol, atropine, staurosporine, genistein, AMP-PNP, and other standard reagents were purchased from Sigma (St. Louis, MO). BAPTA and 5,5'-dinitro-BAPTA were purchased from Molecular Probes (Eugene, OR). CAIN, okadaic acid, pertussis toxin, quinacrine, U-73122, and U-73343 were purchased from Calbiochem (La Jolla, CA). Expression plasmids were generously provided by Drs. T. Snutch and G. Zamponi ($\text{Ca}_v1.2c$; $\alpha 2\delta b$), T. Tanabe ($\text{Ca}_v1.2a$; $\alpha 2\delta a$), D. Lipscombe ($\text{Ca}_v1.3$), V. Flockerzi ($\beta 2a$), K. Campbell ($\beta 3$), D. Yue and E. Peralta (M2 receptor), S. Ikeda (EGFP-RGS2) and R. Fisher (RGS3T; $\beta ARK1ct$; M1 receptor), or were obtained from the Guthrie Institute, Sayre, PA ($G\alpha t$; RGS2; M3, M4 and M5 receptors).

RESULTS

Reconstituted slow muscarinic inhibition of a neuronal L-type Ca^{2+} channel

Fig. 1 illustrates slow muscarinic inhibition of $\text{Ca}_v1.2c$ reconstituted in HEK293 cells. Application of a saturating concentration of carbachol (CCh; 1 mM) triggered profound inhibition of the expressed L-type Ca^{2+} current (Fig. 1 *a*). During steady-state inhibition, current amplitudes were reduced by $62 \pm 3\%$ (mean \pm SEM; $n = 35$). The smaller, inhibited current activated with slightly slower kinetics (Fig. 1 *a, right*), but this probably reflects a decrease in Ca^{2+} -dependent channel inactivation due to the smaller current amplitude, rather than voltage-dependent, G protein-

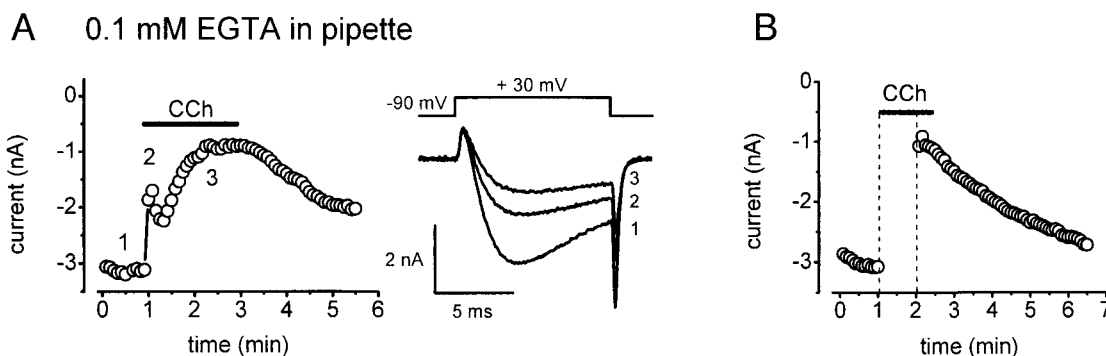


FIGURE 2 Slow muscarinic inhibition does not require Ca^{2+} release from internal stores or influx of extracellular Ca^{2+} . Data from cells coexpressing $\text{Ca}_v1.2\text{c}$ and M1 receptors. (a, left panel) Experiment with low (0.1 mM) EGTA in the pipette solution. $C = 46$ pF; $R_s = 0.7$ M Ω ; $VE = 2.3$ mV. (a, right panel) Ca^{2+} currents recorded at times indicated at left. (b) During the initial 60 s of CCh application (dashed vertical lines), Ca^{2+} currents were not evoked and the membrane potential was clamped at -90 mV. $C = 23$ pF; $R_s = 3.8$ M Ω ; $VE = 11.6$ mV.

mediated channel inhibition (see below). As seen in Fig. 1 a, left, both the onset and the recovery from CCh-mediated inhibition were slow. In a subset of experiments in which CCh was rapidly applied (solution exchange complete within 2 s), the half-time for onset of inhibition was 13 ± 2 s ($n = 6$). Inhibition was prevented ($2 \pm 2\%$, $n = 5$) by simultaneous application of 1 mM atropine and CCh. Furthermore, CCh failed to elicit modulation of $\text{Ca}_v1.2\text{c}$ currents ($0 \pm 0\%$, $n = 4$) in cells not transfected with receptor cDNA. These results show that channel inhibition was mediated through the cotransfected M1 muscarinic acetylcholine receptors.

In rodent SCG neurons, muscarinic receptors mediate voltage-independent inhibition of endogenous L-type Ca^{2+} channels (Mathie et al., 1992). To determine whether reconstituted slow inhibition of $\text{Ca}_v1.2\text{c}$ was similarly voltage-independent, we measured current-voltage (I - V) relationships before and during CCh application. As shown in Fig. 1 b, the averaged I - V relationship was unchanged during slow inhibition. To further test for a change in voltage-dependence, I - V data were converted to conductance-voltage data and fit by a Boltzmann function to obtain estimates of $V_{1/2}$, the midpoint of activation. As illustrated for a representative cell (Fig. 1 c), conductance-voltage relationships were basically unaffected during slow inhibition. Thus, $V_{1/2}$ was 19.6 ± 1.3 mV before applying CCh and 23.3 ± 2.0 mV during the height of slow inhibition ($p = 0.096$, paired t -test; $n = 8$). We also looked for "kinetic slowing" and "prepulse facilitation," two defining features of the voltage-dependent form of Ca^{2+} channel inhibition (Elmslie et al., 1990). As depicted in Fig. 1 d, currents did not exhibit noticeable kinetic slowing during application of CCh. Furthermore, in seven of seven cells currents were decreased in amplitude, rather than facilitated, following a prepulse to $+100$ mV. Prepulses produced similar effects before and during slow inhibition (Fig. 1 d). Altogether, the above data suggest that reconstituted slow muscarinic inhibition of $\text{Ca}_v1.2\text{c}$ is voltage-independent.

In rodent SCG neurons, slow muscarinic inhibition of native L-type Ca^{2+} channels is mediated solely by M1 receptors (Bernheim et al., 1992; Shapiro et al., 1999). Can the slow inhibitory pathway also be activated by other muscarinic receptor subtypes? To address this question, we coexpressed $\text{Ca}_v1.2\text{c}$ with M2, M3, M4, or M5 receptors. As summarized in Fig. 1 e, M3 and M5 receptors also triggered profound inhibition of $\text{Ca}_v1.2\text{c}$. On average, currents were inhibited by $61 \pm 4\%$ ($n = 12$) through M3 receptors and by $67 \pm 8\%$ ($n = 5$) through M5 receptors. Additionally, inhibition of $\text{Ca}_v1.2\text{c}$ through M3 and M5 receptors was kinetically slow. In experiments where CCh was rapidly applied, slow inhibition developed with a half-time of 13 ± 1 s ($n = 3$) for M3 receptors and 11 ± 1 s ($n = 3$) for M5 receptors, not different from inhibition through M1 receptors ($p = 0.7$, ANOVA). These experiments suggest that each of the three Gaq/11 -coupled muscarinic receptor subtypes (M1, M3, and M5) is capable of activating the slow inhibitory pathway. In contrast, no significant modulation of $\text{Ca}_v1.2\text{c}$ was produced through activation of coexpressed M2 or M4 receptors (Fig. 1 e). To confirm functional expression of the latter two receptor subtypes, we coexpressed them with non-L-type Ca^{2+} channels. M2 and M4 receptors each generated strong modulation of $\text{Ca}_v2.2$ and $\text{Ca}_v2.3$ channels (Melliti et al., 1999; Meza et al., 1999; and data not shown).

Like other L-type channels, $\text{Ca}_v1.2\text{c}$ exhibits Ca^{2+} -dependent inactivation (Charnet et al., 1994) which can be triggered either by influx of extracellular Ca^{2+} or by Ca^{2+} released from intracellular stores. We used two separate approaches to determine whether Ca^{2+} -dependent inactivation contributed to slow muscarinic inhibition in our experiments. In the first approach, we switched to a pipette solution containing reduced (0.1 mM) EGTA, under the assumption that reduced Ca^{2+} buffering should produce enhanced Ca^{2+} -dependent inactivation. As shown in Fig. 2 a, CCh evoked an additional fast and transient component of inhibition under these conditions. The amplitude of this fast

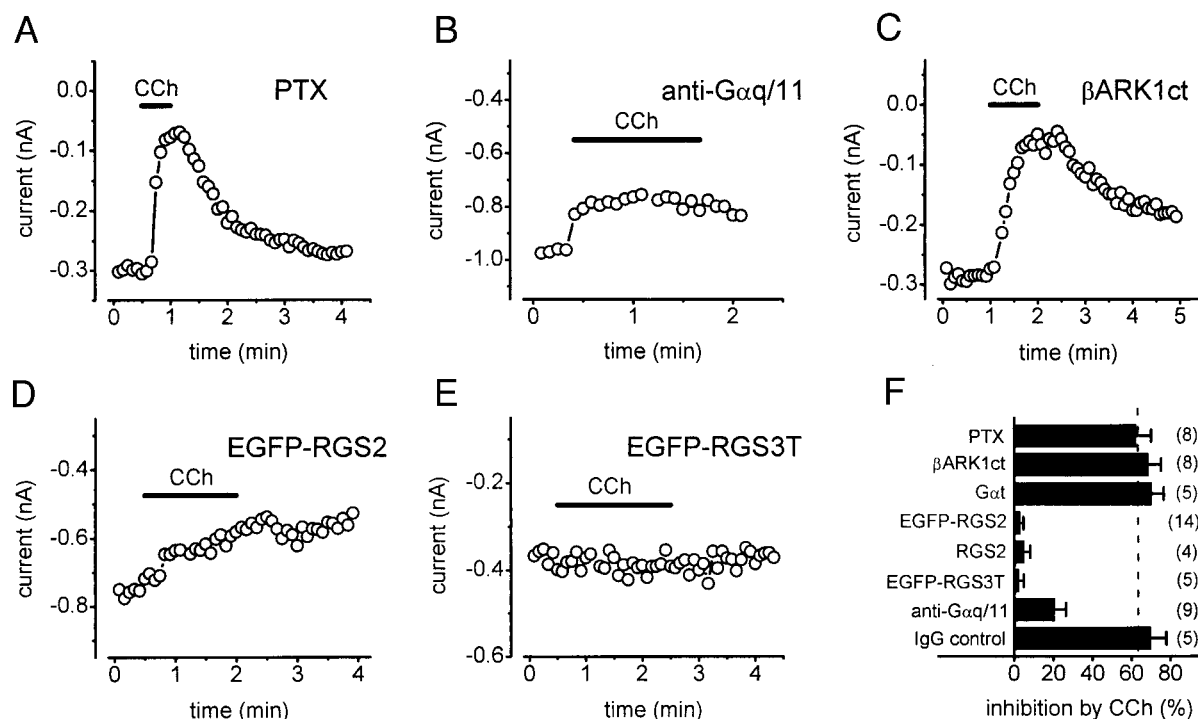


FIGURE 3 Slow muscarinic inhibition is mediated by $\text{G}\alpha\text{q}/11$ and is blocked by RGS proteins. Data from cells coexpressing $\text{Ca}_v1.2\text{c}$ and M1 receptors. (a) Cells were incubated with PTX ($1 \mu\text{g ml}^{-1}$) for at least 4 h before recording. $C = 18 \text{ pF}$; $R_s = 3.7 \text{ M}\Omega$; $V_E = 1.1 \text{ mV}$. (b) Slow inhibition is attenuated by antibodies directed against $\text{G}\alpha\text{q}/11$. Before CCh was applied, cells were dialyzed for 2–10 min with a pipette solution containing a 1:100 dilution ($2 \text{ ng } \mu\text{l}^{-1}$) of a polyclonal antibody directed against a peptide (19 amino acids in length) found within the extreme carboxyl-terminus of $\text{G}\alpha\text{q}/11$. $C = 14 \text{ pF}$; $R_s = 8.5 \text{ M}\Omega$; $V_E = 8.2 \text{ mV}$. (c) Data from a cell coexpressing βARK1ct . $C = 25 \text{ pF}$; $R_s = 2.1 \text{ M}\Omega$; $V_E = 4.6 \text{ mV}$. (d) Data from a cell coexpressing EGFP-RGS2. $C = 18 \text{ pF}$; $R_s = 3.3 \text{ M}\Omega$; $V_E = 2.4 \text{ mV}$. (e) Data from a cell coexpressing EGFP-RGS3T. $C = 85 \text{ pF}$; $R_s = 1.1 \text{ M}\Omega$; $V_E = 0.5 \text{ mV}$. (f) Summary. Data labeled “RGS2” are from cells transfected with untagged RGS2 (i.e., not fused to EGFP). Data labeled “IgG control” are from cells dialyzed through the pipette for 8 min or longer with a 1:100 dilution ($2 \text{ ng } \mu\text{l}^{-1}$) of preimmune rabbit IgG. Dashed vertical line indicates average inhibition in control cells (cf. Fig. 1). Error bars represent $\pm \text{SEM}$.

component was quite variable from cell to cell, ranging from 32 to 77% ($55 \pm 6\%$, $n = 9$). The time course of the fast component closely resembled that of Ca^{2+} transients recorded from tsA201 cells expressing M1 receptors (Shapiro et al., 2000). One explanation for this fast component is Ca^{2+} -dependent inactivation of $\text{Ca}_v1.2\text{c}$ in response to intracellular Ca^{2+} release. However, it is important to note that slow muscarinic inhibition of $\text{Ca}_v1.2\text{c}$ was unchanged in recordings made with low EGTA (Fig. 2a). For example, the kinetically distinct slow phase accounted for $57 \pm 5\%$ ($n = 9$) inhibition of $\text{Ca}_v1.2\text{c}$ in these experiments, indistinguishable from results obtained with the standard (10 mM EGTA) pipette solution (Fig. 1, a and e). These results suggest that release of intracellular Ca^{2+} is not required for slow muscarinic inhibition of $\text{Ca}_v1.2\text{c}$. In the second approach, cells were continuously clamped at -90 mV during the initial 60 s of CCh application. As illustrated in Fig. 2b, robust channel inhibition developed during this interval, in the absence of evoked inward Ca^{2+} currents. Altogether, $\text{Ca}_v1.2\text{c}$ currents were inhibited by $69 \pm 12\%$ ($n = 3$) while cells were continuously clamped at -90 mV , not different from the inhibition that develops while Ca^{2+} currents are

evoked every 5 s (Fig. 1a and e). Thus, slow muscarinic inhibition does not require Ca^{2+} influx through $\text{Ca}_v1.2\text{c}$ channels. Taken together, these experiments indicate that Ca^{2+} -dependent inactivation does not contribute to slow muscarinic inhibition of $\text{Ca}_v1.2\text{c}$ (see also Discussion).

Slow muscarinic inhibition is mediated by $\text{G}\alpha\text{q}/11$

M1 receptors preferentially couple to pertussis toxin (PTX)-insensitive G proteins of the $\text{G}\alpha\text{q}/11$ subfamily (Felder, 1995). To confirm exclusive coupling of M1 receptors to PTX-insensitive G proteins in our experiments, we incubated cells with PTX ($1 \mu\text{g ml}^{-1}$) for 4–6 h before experiments. As shown in Fig. 3, a and f, pretreatment with PTX had no effect on inhibition of $\text{Ca}_v1.2\text{c}$ through M1 receptors. Altogether, CCh inhibited the current by $63 \pm 8\%$ in eight PTX-treated cells, compared with $62 \pm 3\%$ inhibition in 35 untreated control cells. Thus, slow inhibition of $\text{Ca}_v1.2\text{c}$ was mediated by PTX-insensitive G proteins.

To examine whether $\text{G}\alpha\text{q}/11$ or another PTX-insensitive G protein is responsible for slow muscarinic inhibition of

Ca_v1.2c, we dialyzed cells with a polyclonal antibody directed against the extreme carboxyl-termini of Gαq and Gα11. This antibody uncouples signaling through Gαq/11-coupled thromboxane A₂ receptors (Shenker et al., 1991) and attenuates Gαq/11-mediated muscarinic inhibition of endogenous M-type K⁺ channels in rat SCG neurons (Caulfield et al., 1994). As shown in Fig. 3 *b*, anti-Gαq/11 significantly reduced inhibition of Ca_v1.2c through M1 receptors. Thus, CCh elicited only 21 ± 6% (*n* = 9) inhibition in cells dialyzed with anti-Gαq/11, compared with 70 ± 8% (*n* = 5) inhibition in cells dialyzed with preimmune rabbit IgG (Fig. 3 *f*). Anti-Gαq/11 appeared to have a stronger blocking effect in cells dialyzed for longer periods of time; however, due to variations in pipette-cell access resistance it was difficult to establish a tight correlation between length of dialysis and effectiveness of the antibody. The residual CCh-mediated inhibition noted in some cells (e.g., Fig. 3 *b*) is probably attributable to incomplete dialysis with anti-Gαq/11 rather than to the involvement of another G protein. Altogether, these results strongly imply that heterotrimeric Gαq/11 proteins mediate slow muscarinic inhibition of Ca_v1.2c.

Under similar experimental conditions, M1 receptors in rat SCG neurons inhibit endogenous N-type Ca²⁺ channels through a voltage-independent pathway that involves signaling by both Gαq/11 and Gβγ subunits (Kammermeier et al., 2000). To determine whether the voltage-independent inhibition of Ca_v1.2c studied here (Fig. 1, *b–d*) also requires signaling by both Gαq/11 and Gβγ, we expressed the carboxyl-terminal region of β-adrenergic receptor kinase 1 (βARK1ct), which sequesters free Gβγ subunits (Koch et al., 1994), including those released through activation of M1 receptors (Melliti et al., 2000). As shown in Fig. 3 *c*, neither the kinetics nor the magnitude of slow inhibition were significantly altered by coexpressing βARK1ct. Inhibition was similarly unaffected by coexpressing Gat (Fig. 3 *f*), which also strongly buffers free Gβγ subunits (Federman et al., 1992; Kammermeier and Ikeda, 1999). These results indicate that slow muscarinic inhibition of Ca_v1.2c does not require signaling by Gβγ.

Slow muscarinic inhibition is blocked by RGS2 and RGS3T

Regulators of G-protein signaling (RGS proteins) function as GTPase-accelerating proteins (GAPs) and/or as effector antagonists for certain classes of Gα subunits (Berman and Gilman, 1998). Previous studies have demonstrated that RGS proteins can influence the G protein-dependent modulation of N-type, P/Q-type, and R-type Ca²⁺ channels (Jeong and Ikeda, 1998; Diversé-Pierluissi et al., 1999; Melliti et al., 1999, 2000, 2001; Kammermeier et al., 2000; Mark et al., 2000). However, no previous work has shown that RGS proteins influence L-type channel modulation. Both RGS2 and RGS3T are known to antagonize signaling

by Gαq/11 (Heximer et al., 1997; Chatterjee et al., 1997; Scheschonka et al., 2000). As illustrated in Fig. 3, *d–f*, slow muscarinic inhibition of Ca_v1.2c was effectively blocked by coexpressing either EGFP-RGS2 or EGFP-RGS3T. Identical results were obtained with untagged RGS2 (Fig. 3 *f*). In separate experiments (not shown), we found that RGS2 also blocked slow muscarinic inhibition of Ca_v1.2c through M3 or M5 receptors. Together with our antibody experiments (Fig. 3, *b* and *f*), these results support the conclusion that Gαq/11 activates the slow muscarinic pathway in HEK293 cells (see also Delmas et al., 1998; Haley et al., 2000). Additionally, these findings suggest that certain RGS proteins may antagonize slow muscarinic inhibition of L-type channels in native cells.

Slow muscarinic inhibition does not appear to involve phospholipase C or phospholipase A₂

Phospholipase C-β1 (PLC-β1) is the principal downstream effector enzyme of Gαq/11 (Smrcka et al., 1991). In the canonical signaling pathway, PLC-β1 cleaves phosphatidylinositol-4,5-bisphosphate (PIP₂) into inositol trisphosphate (IP₃) and 1,2-diacylglycerol (DAG). IP₃ triggers Ca²⁺ release from intracellular stores (Berridge, 1993), whereas DAG activates both conventional and novel isozymes of protein kinase C (Mellor and Parker, 1998). We used the aminosteroid U-73122 to test for involvement of PLC in slow muscarinic inhibition of Ca_v1.2c. In support of a previous report by Macrez-Lepretre et al. (1996), we observed that U-73122 strongly blocked Ca_v1.2c currents when applied extracellularly. To circumvent this problem, U-73122 was applied in the pipette solution. Altogether, in cells dialyzed with 10 μM U-73122 for at least 8 min, CCh still inhibited the Ca²⁺ current by 46 ± 6% (*n* = 10). Because CCh produced similar inhibition (39 ± 11%; *n* = 3) in cells dialyzed for equivalent times with 10 μM U-73343, the inactive analog of U-73122, we conclude that the weak effects of these compounds are nonspecific. We also used quinacrine to assess the potential involvement of phospholipase A₂ (PLA₂). In five cells dialyzed with 100 μM quinacrine for at least 6 min, CCh still inhibited the Ca²⁺ current by 50 ± 5%. From these results, we conclude that slow muscarinic inhibition of Ca_v1.2c is unlikely to involve PLC or PLA₂.

Slow muscarinic inhibition does not appear to involve protein phosphorylation or dephosphorylation

We used several pharmacological tools to further characterize the pathway responsible for slow muscarinic inhibition of Ca_v1.2c. As illustrated in Fig. 4 *a*, slow inhibition was undiminished by 100 nM staurosporine, which inhibits protein kinase A, protein kinase C, protein kinase G, Ca²⁺/

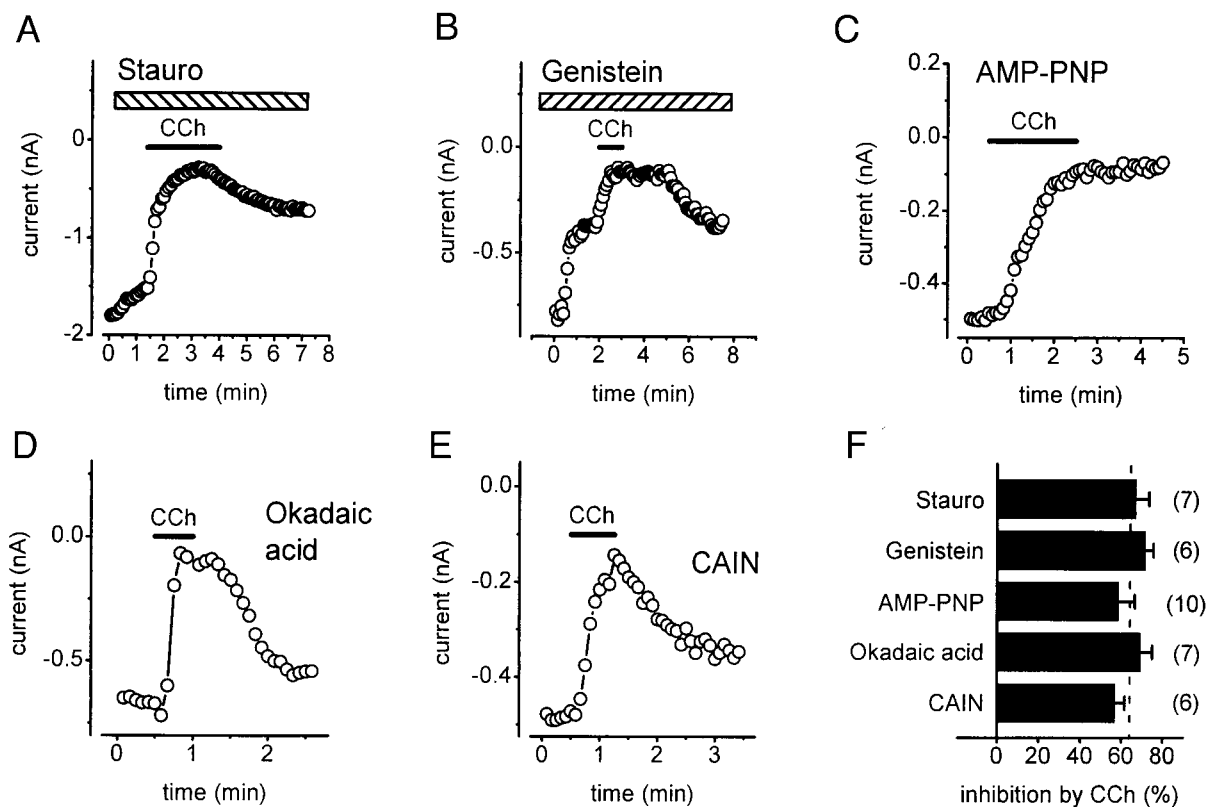


FIGURE 4 Slow muscarinic inhibition does not appear to involve protein kinases or phosphatases. Data from cells coexpressing $\text{Ca}_v1.2c$ and M1 receptors. (a) Cells were exposed to 100 nM staurosporine (Stauro) dissolved in the bath solution. Staurosporine application is indicated by a hatched horizontal bar. $C = 25$ pF; $R_s = 5.7$ M Ω ; $VE = 8.7$ mV. (b) Cells were exposed to 100 μM genistein dissolved in the bath solution. Genistein application is indicated by a hatched horizontal bar. $C = 47$ pF; $R_s = 2.2$ M Ω ; $VE = 1.8$ mV. (c) Cells were dialyzed with the standard pipette solution, modified to contain 5 mM AMP-PNP in place of MgATP, for at least 5 min before applying CCh. $C = 22$ pF; $R_s = 3.4$ M Ω ; $VE = 1.7$ mV. (d) Cells were exposed to 50 nM okadaic acid for at least 2 h before and during experiments. $C = 27$ pF; $R_s = 8.6$ M Ω ; $VE = 4.9$ mV. (e) Cells were dialyzed with the standard pipette solution containing 10 μM calcineurin autoinhibitory peptide (CAIN) for at least 6 min before applying CCh. $C = 18$ pF; $R_s = 10.8$ M Ω ; $VE = 5.2$ mV. (f) Summary. Dashed vertical line indicates average inhibition in control cells. Error bars represent \pm SEM.

calmodulin-activated protein kinases, and some members of the Src family of tyrosine kinases (Hanke et al., 1996). On average, CCh inhibited Ca^{2+} currents by $67 \pm 6\%$ ($n = 7$) in staurosporine-treated cells, not different from controls. Slow inhibition was also undiminished by 100 μM genistein, a broad-spectrum inhibitor of protein tyrosine kinases. As previously reported for other Ca^{2+} channels (Meza et al., 1999), genistein alone strongly reduced Ca^{2+} currents (Fig. 4 b). This effect may be due to inhibition of basally active tyrosine kinases or (more likely) direct channel block. Once current amplitudes had stabilized in the continued presence of genistein, CCh produced $72 \pm 4\%$ ($n = 6$) inhibition, similar to controls. These data suggest that slow muscarinic inhibition does not involve serine/threonine kinases or tyrosine kinases.

As shown in Fig. 4 c, robust slow muscarinic inhibition of $\text{Ca}_v1.2c$ persisted in cells dialyzed with a pipette solution containing nonhydrolyzable AMP-PNP (5 mM) in place of ATP. On average, inhibition was $52 \pm 7\%$ ($n = 10$) in AMP-PNP-dialyzed cells. This result suggests that phos-

phorylation is not required for slow inhibition. The onset of inhibition appeared somewhat slower in AMP-PNP-dialyzed cells (Fig. 4 c) than in control cells, but this possible effect was not pursued. However, inhibition was clearly irreversible in cells dialyzed with AMP-PNP (Fig. 4 c). For example, whereas Ca^{2+} currents recovered by $66 \pm 10\%$ ($n = 14$) following CCh washout in control cells, currents in AMP-PNP-dialyzed cells recovered by only $6 \pm 4\%$ ($n = 10$). This significant difference ($p < 0.0001$) suggested that phosphorylation might be required for recovery from slow inhibition—in this case, the onset of slow inhibition would reflect dephosphorylation. To assess this possibility we used okadaic acid, which inhibits protein phosphatases PP1, PP2A, PP4, PP5, and PP6 at relatively low concentrations (Herzig and Neumann, 2000). Cells were exposed to 50 nM okadaic acid in the culture medium for 2 h before experiments, and the same concentration of okadaic acid was continuously present in the bath solution. We also performed experiments in which 10 μM CAIN, a specific inhibitor of PP2B (calcineurin), was added to the pipette

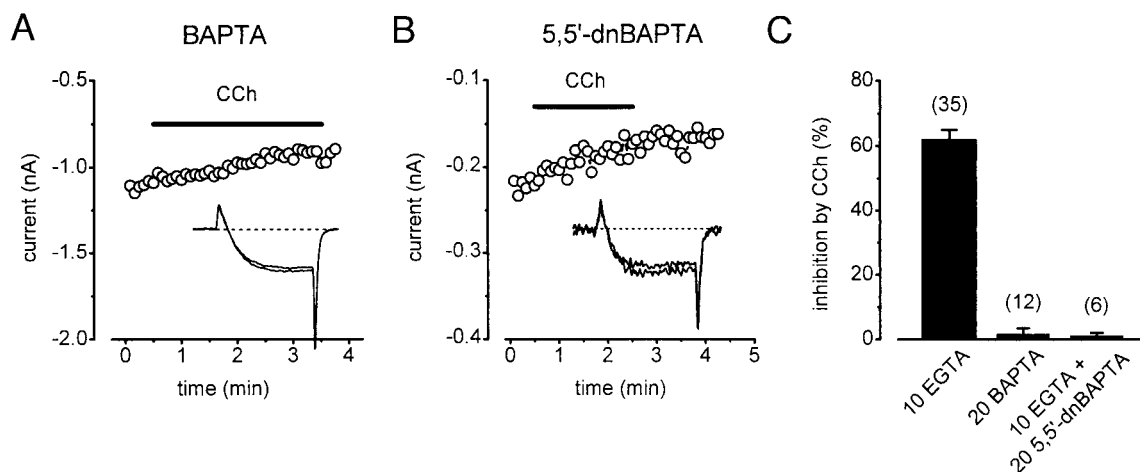


FIGURE 5 Slow muscarinic inhibition is blocked by BAPTA and 5,5'-dinitro-BAPTA. Data from cells coexpressing $\text{Ca}_v1.2c$ and M1 receptors. (a) Cells were dialyzed with a pipette solution containing 20 mM BAPTA for at least 5 min before recording Ca^{2+} currents. The inset shows Ca^{2+} currents recorded before and during exposure to 1 mM CCh. $C = 14$ pF; $R_s = 4.2$ M Ω ; $VE = 4.6$ mV. (b) Cells were dialyzed with a pipette solution containing 5,5'-dinitro-BAPTA (20 mM) plus EGTA (10 mM) for at least 5 min before recording Ca^{2+} currents. The inset shows Ca^{2+} currents recorded before and during exposure to 1 mM CCh. $C = 19$ pF; $R_s = 3.8$ M Ω ; $VE = 0.8$ mV. (c) Summary. Control data (10 EGTA) from Fig. 1 *e* are included for comparison. Error bars represent \pm SEM.

solution. CAIN has been previously used to block dopaminergic inhibition of native L-type Ca^{2+} channels in striatal neurons (Hernández-López et al., 2000). As shown in Fig. 4, *d* and *e*, neither phosphatase inhibitor decreased slow muscarinic inhibition of $\text{Ca}_v1.2c$. On average, CCh produced $69 \pm 6\%$ ($n = 7$) inhibition in cells exposed to okadaic acid and $57 \pm 5\%$ ($n = 6$) inhibition in cells dialyzed with CAIN (Fig. 4*f*). We cannot account for the apparent irreversibility of slow inhibition in cells dialyzed with AMP-PNP. However, taken together, our results suggest that slow muscarinic inhibition does not involve protein phosphorylation or dephosphorylation.

BAPTA blocks slow muscarinic inhibition independently of Ca^{2+} chelation

Previous studies have found that high intracellular concentrations of BAPTA disrupt slow muscarinic inhibition of native L-type Ca^{2+} currents in rat SCG neurons (Mathie et al., 1992) and striatal neurons (Howe and Surmeier, 1995). In the present experiments, we found that a pipette solution containing 20 mM BAPTA completely blocked inhibition of $\text{Ca}_v1.2c$ through M1 receptors (Fig. 5 *a*). Thus, CCh inhibited $\text{Ca}_v1.2c$ currents by only $2 \pm 2\%$ ($n = 12$) in BAPTA-dialyzed cells. However, because BAPTA may have actions unrelated to Ca^{2+} chelation (Beech et al., 1991; Meza et al., 1999), we also performed experiments in which cells were dialyzed with a pipette solution containing 5,5'-dinitro-BAPTA (20 mM). This latter molecule has a much lower affinity for Ca^{2+} ($K_d = 7$ mM) than regular BAPTA ($K_d = 165$ nM). The pipette solution containing 5,5'-dinitro-BAPTA also included 10 mM EGTA to buffer

intracellular Ca^{2+} at the same concentration as in control cells. Significantly, 5,5'-dinitro-BAPTA blocked muscarinic inhibition of $\text{Ca}_v1.2c$ as effectively as BAPTA (Fig. 5 *b*). On average, CCh produced only $1 \pm 1\%$ inhibition in cells dialyzed with 5,5'-dinitro-BAPTA ($n = 6$). These results show that BAPTA blocks slow muscarinic inhibition of L-type Ca^{2+} channels reconstituted in HEK293 cells, as it does in rat SCG neurons (Mathie et al., 1992) and striatal neurons (Howe and Surmeier, 1995). However, the effect of 5,5'-dinitro-BAPTA indicates that Ca^{2+} chelation is not the mechanism by which BAPTA blocks slow muscarinic inhibition.

Other L-type Ca^{2+} channels also undergo slow muscarinic inhibition

To determine whether slow muscarinic inhibition is an exclusive property of $\text{Ca}_v1.2c$ or a more general characteristic of L-type channels, we cotransfected cells with M1 receptors and $\text{Ca}_v1.2a$, the cardiac splice-variant of $\text{Ca}_v1.2$. $\text{Ca}_v1.2a$ was coexpressed with ancillary $\beta 2a$ (cardiac) and $\alpha 2\delta a$ (skeletal muscle) subunits. As shown in Fig. 6 *a*, $\text{Ca}_v1.2a$ was substantially inhibited ($66 \pm 7\%$; $n = 8$) through M1 receptors. The speed of onset and recovery from inhibition closely resembled that of the neuronal splice-variant $\text{Ca}_v1.2c$ (see Fig. 1 *a*). These results suggest that neuronal and cardiac splice-variants of $\text{Ca}_v1.2$ can both be inhibited through a slow muscarinic pathway. Furthermore, the identity of the ancillary subunits does not appear to be critical; slow inhibition occurred when either $\beta 2a/\alpha 2\delta a$ or $\beta 3/\alpha 2\delta b$ subunits were expressed.

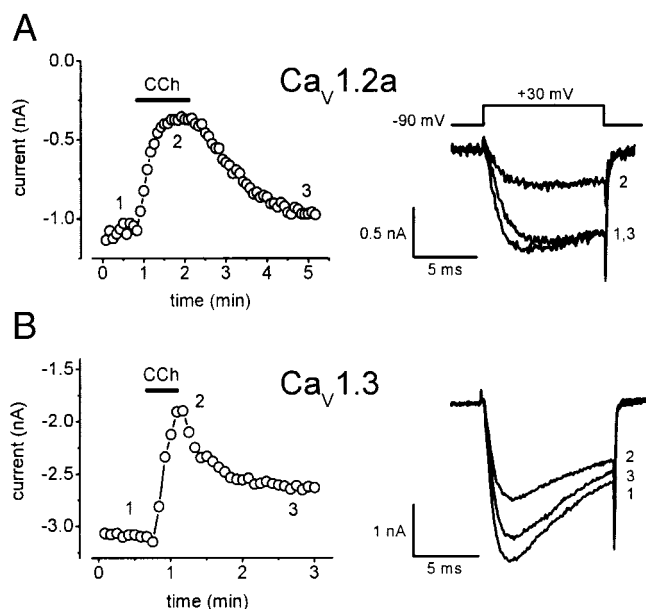


FIGURE 6 Cardiac $\text{Ca}_v1.2a$ and neuronal/neuroendocrine $\text{Ca}_v1.3$ channels also undergo slow muscarinic inhibition. (a) Time-plot of slow muscarinic inhibition in a cell coexpressing M1 receptors, cardiac $\text{Ca}_v1.2a$, skeletal muscle $\alpha 2\delta a$, and cardiac $\beta 2a$ channel subunits. $C = 58$ pF; $R_s = 1.1$ M Ω ; $VE = 1.2$ mV. (b) Time-plot of slow muscarinic inhibition in a cell coexpressing M1 receptors and neuronal $\text{Ca}_v1.3$, $\alpha 2\delta b$, and $\beta 3$ channel subunits. $C = 16$ pF; $R_s = 2.9$ M Ω ; $VE = 9.2$ mV.

We next examined modulation of $\text{Ca}_v1.3$, which represents a distinct family of neuronal/neuroendocrine L-type channels. For these experiments we used a splice-variant (+11/ $\Delta 32/42a$) of $\text{Ca}_v1.3$ cloned from rat SCG neurons (Xu and Lipscombe, 2001). As illustrated in Fig. 6 b, $\text{Ca}_v1.3$ was robustly inhibited through M1 receptors. On average, CCh produced $48 \pm 5\%$ inhibition of $\text{Ca}_v1.3$ currents ($n = 16$). Both the onset and recovery from inhibition were slow, very similar to $\text{Ca}_v1.2a$ and $\text{Ca}_v1.2c$. These results suggest that both $\text{Ca}_v1.2$ and $\text{Ca}_v1.3$ Ca^{2+} channel families are inhibited through a slow muscarinic pathway. Therefore, slow muscarinic inhibition appears to be a general characteristic of L-type Ca^{2+} channels.

DISCUSSION

We have reconstituted slow muscarinic inhibition of L-type Ca^{2+} channels in HEK293 cells. Reconstituted inhibition of $\text{Ca}_v1.2c$ closely resembles slow muscarinic inhibition of endogenous L-type Ca^{2+} channels in central and peripheral neurons (Mathie et al., 1992; Howe and Surmeier, 1995; Stewart et al., 1999). Our present findings complement and extend previous studies indicating that slow muscarinic inhibition of cloned M-type K^+ channels (Shapiro et al., 2000) and cloned N-type Ca^{2+} channels (Melliti et al., 2001) can be faithfully reproduced in non-neuronal cells. The overall similarity between slow muscarinic inhibition in

HEK293 cells and neurons strongly suggests that the underlying signaling pathway is present in both cell types. The ability to reconstitute slow muscarinic inhibition in heterologous systems should be helpful in further elucidating the molecular components of this signaling pathway.

M1 receptors are solely responsible for mediating slow muscarinic inhibition of L-type and N-type Ca^{2+} channels and M-type K^+ channels in rodent SCG neurons (Hamilton et al., 1997; Shapiro et al., 1999). However, M1 receptors are not required for muscarinic suppression of M-type K^+ currents in pyramidal neurons (Rouse et al., 2000) or in CA1 or CA3 neurons of mouse hippocampus (Fisahn et al., 2002). We found that all three $\text{G}\alpha_q/11$ -coupled muscarinic receptors (M1, M3, and M5) could trigger slow inhibition of $\text{Ca}_v1.2c$ (Fig. 1 e). These findings support the idea that M3 and M5 receptors activate the slow muscarinic inhibitory pathway in some cell types in vivo.

$\text{G}\alpha_i/o$ -coupled M2 and M4 receptors failed to modulate $\text{Ca}_v1.2c$ channels in our experiments (Fig. 1 e). In a previous study, Pemberton and Jones (1997) reported that M2 and M4 receptors inhibited endogenous L-type Ca^{2+} channel currents in a mouse embryonic fibroblast cell line (NIH 3T3). In their experiments, channel inhibition through M2 and M4 receptors was PTX-sensitive and thus clearly different from slow muscarinic inhibition of $\text{Ca}_v1.2c$ in our experiments (Fig. 3 a). Pemberton and Jones (1997) also concluded that channel inhibition through M1 receptors was mediated by protein kinase C. In contrast, our present results (Fig. 4) indicate that protein kinases are not involved in slow muscarinic inhibition of $\text{Ca}_v1.2c$. One difficulty in comparing our results with those of Pemberton and Jones (1997) is that the molecular identity of the channels they studied was not known. Possibly, those L-type channels differ structurally from $\text{Ca}_v1.2a$, $\text{Ca}_v1.2c$, and $\text{Ca}_v1.3$ and are consequently modulated by different mechanisms. Another possibility is that muscarinic receptors activate different signaling pathways in NIH 3T3 and HEK293 cells.

Slow muscarinic inhibition of $\text{Ca}_v1.2c$ was not enhanced by lowering the concentration of EGTA in the pipette solution (Fig. 2 a). This result indicates that slow inhibition does not involve Ca^{2+} release from intracellular stores, in agreement with a previous demonstration that intracellular Ca^{2+} transients are not required for slow muscarinic inhibition of endogenous M-type K^+ channels in SCG neurons (Cruzblanca et al., 1998). It is noteworthy, however, that CCh elicited an additional fast and transient component of inhibition in recordings made with low EGTA (Fig. 2 a). Thus, under physiological conditions $\text{G}\alpha_q/11$ -coupled receptors may trigger fast and transient Ca^{2+} -dependent inhibition of L-type channels in addition to triggering slow and sustained Ca^{2+} -independent inhibition.

Our results also indicate that slow muscarinic inhibition does not require Ca^{2+} influx through L-type channels (Fig. 2 b). This finding agrees with Mathie et al. (1992), who used cell-attached recordings to study slow muscarinic inhibition

of endogenous L-type channels in rat SCG neurons. In their experiments, the bath was nominally Ca²⁺-free and the pipette contained 110 mM Ba²⁺ as the sole divalent cation. Under those conditions, Ca²⁺ influx through membrane channels should be minimal. Although Ca²⁺-dependent inactivation is a prominent feature of L-type Ca²⁺ channels (cf. Adams and Tanabe, 1997), this phenomenon requires significant Ca²⁺ influx or Ca²⁺ release from internal sources. Since blocking Ca²⁺ release or influx (Fig. 2) did not prevent slow muscarinic inhibition, we conclude that Ca²⁺-dependent inactivation does not contribute to slow muscarinic inhibition of L-type channels.

Recent studies demonstrate that RGS proteins can influence G protein-dependent modulation of neuronal N-type, P/Q-type, and R-type Ca²⁺ channels (Jeong and Ikeda, 1998; Diversé-Pierluissi et al., 1999; Melliti et al., 1999, 2000, 2001; Kammermeier et al., 2000; Mark et al., 2000). In the present work, RGS2 and RGS3T blocked slow muscarinic inhibition of neuronal L-type Ca²⁺ channels (Fig. 3, *d–f*). These findings raise the possibility that by antagonizing the slow muscarinic pathway, certain RGS proteins may influence cellular events (such as gene transcription; Murphy et al., 1991; Bading et al., 1993) that are triggered by Ca²⁺ influx through L-type channels.

Slow muscarinic inhibition of Ca_v1.2c was insensitive to the phospholipase C inhibitor U-73122 and also to the broad-spectrum kinase inhibitor staurosporine (Fig. 4). These results suggest that the slow muscarinic inhibitory pathway does not use phospholipase C or protein kinases, in agreement with previous data from rodent SCG neurons (Bernheim et al., 1991; Cruzblanca et al., 1998) and HEK293 cells (Shapiro et al., 2000; Melliti et al., 2001). However, our results with quinacrine, genistein, okadaic acid, and CAIN provide new information by suggesting that phospholipase A₂, protein tyrosine kinases, and serine/threonine phosphatases are also not involved in the slow muscarinic pathway. Finally, our results with AMP-PNP suggest that phosphorylation is not required for slow muscarinic inhibition.

Sensitivity to BAPTA has been widely cited as a distinguishing characteristic of the slow muscarinic pathway (Beech et al., 1991; Bernheim et al., 1991; Mathie et al., 1992; Howe and Surmeier, 1995; Stewart et al., 1999), and it has been frequently assumed that Ca²⁺ chelation underlies the effects of BAPTA. In an earlier study, Beech et al. (1991) reported that 5,5'-dinitro-BAPTA reduced slow muscarinic inhibition of endogenous N-type Ca²⁺ current in SCG neurons. In the present experiments, we found that 5,5'-dinitro-BAPTA completely blocked slow muscarinic inhibition of Ca_v1.2c (Fig. 5). It is unlikely that Ca²⁺ chelation is responsible for this effect, because 5,5'-dinitro-BAPTA binds Ca²⁺ with relatively low affinity ($K_d = 7$ mM). Based on these and other results (Beech et al., 1991; Meza et al., 1999), we conclude that some property of

BAPTA other than Ca²⁺ buffering interferes with the slow inhibitory pathway.

We found that the cardiac Ca_v1.2a and the neuronal/neuroendocrine Ca_v1.3 channels are also robustly inhibited through M1 receptors (Fig. 6). It seems reasonable to predict that Ca_v1.2a and Ca_v1.3 are inhibited through the same slow, voltage-independent and Gαq/11-mediated pathway that we characterized in detail for Ca_v1.2c, although our present experiments do not establish this point. The apparently similar responses of these three L-type channels to M1 receptors suggests that the molecular determinants of slow muscarinic inhibition may be conserved within Ca_v1.2 and Ca_v1.3 families. However, at the amino acid level Ca_v1.2a is ~95% identical to Ca_v1.2c (Snutch et al., 1991) and Ca_v1.3 is ~70% identical to Ca_v1.2c (Hui et al., 1991; Seino et al., 1992; Williams et al., 1992). Thus, these L-type channels share large regions of homology, making it difficult to identify sequences that could potentially be involved in slow muscarinic inhibition. Further experiments using channels with different sensitivities to slow muscarinic inhibition are needed to reveal the structural basis for this form of channel modulation. Nonetheless, our results with Ca_v1.2a and Ca_v1.3 suggest that slow muscarinic inhibition may be a general characteristic of L-type channels, rather than a unique property of neuronal Ca_v1.2c channels. Ca_v1.2a is essential for excitation-contraction coupling in cardiac muscle cells (Näbauer et al., 1989), and Ca_v1.3 is required for normal sinoatrial node pacemaker activity and for hearing (Platzer et al., 2000). Thus, slow muscarinic inhibition of different L-type channels may influence Ca²⁺ influx in a wide variety of cell types and may play important roles in diverse physiological processes.

We thank the Guthrie Institute and numerous colleagues for generously providing expression plasmids. We also thank Dr. U. Meza for helpful comments on the manuscript.

This work was supported by grants from the National Institutes of Health (NS34423), the American Heart Association (0040067N), and the Utah Agricultural Experimental Station (Project 638) to B.A.A., and by a Pre-doctoral Fellowship from the American Heart Association (9910094Z) to R.A.B.

REFERENCES

- Adams, B. A., and T. Tanabe. 1997. Structural regions of the cardiac Ca channel α_{1C} subunit involved in Ca-dependent inactivation. *J. Gen. Physiol.* 110:379–389.
- Bading, H., D. D. Ginty, and M. E. Greenberg. 1993. Regulation of gene expression in hippocampal neurons by distinct calcium signalling pathways. *Nature*. 260:181–186.
- Beech, D. J., L. Bernheim, and B. Hille. 1991. Intracellular Ca buffers disrupt suppression of Ca²⁺ current and M current in rat sympathetic neurons. *Proc. Natl. Acad. Sci. USA*. 88:652–656.
- Berman, D. M., and A. G. Gilman. 1998. Mammalian RGS proteins: barbarians at the gate. *J. Biol. Chem.* 273:1269–1272.
- Bernheim, L., D. J. Beech, and B. Hille. 1991. A diffusible second messenger mediates one of the pathways coupling receptors to calcium channels in rat sympathetic neurons. *Neuron*. 6:859–867.

- Bernheim, L., A. Mathie, and B. Hille. 1992. Characterization of muscarinic receptor subtypes inhibiting Ca^{2+} current and M current in rat sympathetic neurons. *Proc. Natl. Acad. Sci. USA*. 89:9544–9548.
- Berridge, M. J. 1993. Inositol trisphosphate and calcium signalling. *Nature*. 361:315–325.
- Bourinet, E., T. W. Soong, K. Sutton, S. Slaymaker, E. Mathews, A. Monteil, G. W. Zamponi, J. Nargeot, and T. P. Snutch. 1999. Splicing of α_{1A} subunit gene generates phenotypic variants of P- and Q-type calcium channels. *Nat. Neurosci.* 2:407–415.
- Caulfield, M. P., S. Jones, Y. Vallis, N. J. Buckley, G.-D. Kim, G. Milligan, and D. A. Brown. 1994. Muscarinic M-current inhibition via $\text{Gaq}/11$ and α -adrenoreceptor inhibition of Ca^{2+} current via Gao in rat sympathetic neurones. *J. Physiol.* 477:415–422.
- Charnet, P., E. Bourinet, S. J. Dubel, T. P. Snutch, and J. Nargeot. 1994. Calcium currents recorded from a neuronal α_{1C} L-type calcium channel in *Xenopus* oocytes. *FEBS Lett.* 344:87–90.
- Chatterjee, T. K., A. K. Eapen, and R. A. Fisher. 1997. A truncated form of RGS3 negatively regulates G protein-coupled stimulation of adenylyl cyclase and phosphoinositide phospholipase C. *J. Biol. Chem.* 272:15481–15487.
- Cruzblanca, H., D.-S. Koh, and B. Hille. 1998. Bradykinin inhibits M current via phospholipase C and Ca^{2+} release from IP_3 -sensitive stores in rat sympathetic neurons. *Proc. Natl. Acad. Sci. USA*. 95:7151–7156.
- Delmas, P., F. C. Abogadie, M. Dayrell, J. E. Haley, G. Milligan, M. P. Caulfield, D. A. Brown, and N. J. Buckley. 1998. G-proteins and G-protein subunits mediating cholinergic inhibition of N-type calcium currents in sympathetic neurons. *Eur. J. Neurosci.* 10:1654–1666.
- Diversé-Pierluissi, M. A., T. Fischer, J. D. Jordan, M. Schiff, D. F. Ortiz, M. G. Farquhar, and L. De Vries. 1999. Regulators of G protein signaling proteins as determinants of the rate of desensitization of presynaptic calcium channels. *J. Biol. Chem.* 274:14490–14494.
- Dolphin, A. C. 1999. L-type calcium channel modulation. *Adv. Second Messenger Phosphoprotein Res.* 33:153–177.
- Elmslie, K. S., W. Zhou, and S. W. Jones. 1990. LHRH and GTP- γ -S modify calcium current activation in bullfrog sympathetic neurons. *Neuron*. 5:75–80.
- Federman, A. D., B. R. Conklin, K. A. Schrader, R. R. Reed, and H. R. Bourne. 1992. Hormonal stimulation of adenylyl cyclase through G_i -protein $\beta\gamma$ subunits. *Nature*. 356:159–161.
- Felder, C. C. 1995. Muscarinic acetylcholine receptors: signal transduction through multiple effectors. *FASEB J.* 9:619–625.
- Fisahn, A., M. Yamada, A. Duttaroy, J. W. Gan, C. X. Deng, C. J. McBain, and J. Wess. 2002. Muscarinic induction of hippocampal gamma oscillations requires coupling of the M1 receptor to two mixed cation currents. *Neuron*. 33:615–624.
- Forti, L., and D. Pietrobon. 1993. Functional diversity of L-type calcium channels in rat cerebellar neurons. *Neuron*. 10:437–450.
- Haley, J. E., P. Delmas, S. Offermanns, F. C. Abogadie, M. I. Simon, N. J. Buckley, and D. A. Brown. 2000. Muscarinic inhibition of calcium current and M current in Gaq -deficient mice. *J. Neurosci.* 20:3973–3979.
- Hamilton, S. E., M. D. Loose, M. Qi, A. I. Levey, B. Hille, G. S. McKnight, R. L. Idzerda, and N. M. Nathanson. 1997. Disruption of the m1 receptor gene ablates muscarinic receptor-dependent M current regulation and seizure activity in mice. *Proc. Natl. Acad. Sci. USA*. 94:13311–13316.
- Hanke, J. H., J. P. Gardner, R. L. Dow, P. S. Changelian, W. H. Brissette, E. J. Weringer, B. A. Pollok, and P. A. Connelly. 1996. Discovery of a novel, potent, and Src family-selective tyrosine kinase inhibitor. *J. Biol. Chem.* 271:695–701.
- Hell, J. W., R. E. Westenbroek, C. Warner, M. K. Ahljianian, W. Prystay, M. M. Gilbert, T. P. Snutch, and W. A. Catterall. 1993. Identification of differential subcellular localization of the neuronal class C and class D L-type calcium $\alpha 1$ subunits. *J. Cell Biol.* 123:949–962.
- Hernández-López, S., T. Tkatch, E. Perez-Garci, E. Galarraga, J. Bargas, H. Hamm, and D. J. Surmeier. 2000. D_2 dopamine receptors in striatal medium spiny neurons reduce L-type Ca^{2+} currents and excitability via a novel $\text{PLC}\beta 1$ - IP_3 -calcineurin-signaling cascade. *J. Neurosci.* 20:8987–8995.
- Herzig, S., and J. Neumann. 2000. Effects of serine/threonine protein phosphatases on ion channels in excitable membranes. *Physiol. Rev.* 80:173–210.
- Heximer, S. P., N. Watson, M. E. Linder, K. J. Blumer, and J. R. Hepler. 1997. RGS2/GOS8 is a selective inhibitor of $\text{Gq}\alpha$ function. *Proc. Natl. Acad. Sci. USA*. 94:14389–14393.
- Howe, A. R., and D. J. Surmeier. 1995. Muscarinic receptors modulate N-, P-, and L-type Ca^{2+} currents in rat striatal neurons through parallel pathways. *J. Neurosci.* 15:458–469.
- Hui, A., P. T. Ellinor, O. Krizanov, J.-J. Wang, R. J. Diebold, and A. Schwartz. 1991. Molecular cloning of multiple subtypes of a novel rat brain isoform of the α_1 subunit of the voltage-dependent calcium channel. *Neuron*. 7:35–44.
- Jensen, K., M. S. Jensen, and J. D. C. Lambert. 1999. Role of presynaptic L-type Ca^{2+} channels in GABAergic synaptic transmission in cultured hippocampal neurons. *J. Neurophysiol.* 81:1225–1230.
- Jeong, S.-W., and S. R. Ikeda. 1998. G protein α subunit $\text{G}\alpha_z$ couples neurotransmitter receptors to ion channels in sympathetic neurons. *Neuron*. 21:1201–1212.
- Kammermeier, P. J., and S. R. Ikeda. 1999. Expression of RGS2 alters the coupling of metabotropic glutamate receptor 1a to M-type K^+ and N-type Ca^{2+} channels. *Neuron*. 22:819–829.
- Kammermeier, P. J., V. Ruiz-Velasco, and S. R. Ikeda. 2000. A voltage-independent calcium current inhibitory pathway activated by muscarinic agonists in rat sympathetic neurons requires both $\text{G}\alpha_{q/11}$ and $\text{G}\beta\gamma$. *J. Neurosci.* 20:5623–5629.
- Koch, W. J., B. E. Hawes, J. Inglese, L. Luttrell, and R. J. Lefkowitz. 1994. Cellular expression of the carboxyl terminus of a G protein-coupled receptor kinase attenuates $\text{G}\beta\gamma$ -mediated signalling. *J. Biol. Chem.* 269:6193–6197.
- Macrez-Lepêtre, N., J. L. Morel, and J. Mironneau. 1996. Effects of phospholipase C inhibitors on Ca^{2+} channel stimulation and Ca^{2+} release from intracellular stores evoked by α_{1A} - and α_{2A} -adrenoceptors in rat portal vein myocytes. *Biochem. Biophys. Res. Commun.* 218:30–34.
- Mark, M. D., S. Wittemann, and S. Herlitze. 2000. G protein modulation of recombinant P/Q-type calcium channels by regulators of G protein signalling proteins. *J. Physiol.* 528:65–77.
- Mathie, A., L. Bernheim, and B. Hille. 1992. Inhibition of N- and L-type calcium currents by muscarinic receptor activation in rat sympathetic neurones. *Neuron*. 8:907–914.
- Melliti, K., U. Meza, and B. A. Adams. 2000. Muscarinic stimulation of $\alpha 1E$ Ca channels is selectively blocked by RGS2 and $\text{PLC}\beta 1$ acting as effector antagonists. *J. Neurosci.* 20:7167–7173.
- Melliti, K., U. Meza, and B. A. Adams. 2001. RGS2 blocks slow muscarinic inhibition of N-type Ca^{2+} channels reconstituted in a human cell line. *J. Physiol.* 532:337–347.
- Melliti, K., U. Meza, R. Fisher, and B. A. Adams. 1999. Regulators of G protein signalling attenuate the G protein-mediated inhibition of N-type Ca channels. *J. Gen. Physiol.* 113:97–109.
- Mellor, H., and P. J. Parker. 1998. The extended protein kinase C family. *Biochem. J.* 332:281–292.
- Meza, U., R. A. Bannister, K. Melliti, and B. A. Adams. 1999. Biphasic, opposing modulation of cloned neuronal $\alpha 1E$ Ca channels by distinct signalling pathways coupled to M2 muscarinic acetylcholine receptors. *J. Neurosci.* 19:6806–6817.
- Mikami, A., K. Imoto, T. Tanabe, T. Niidome, Y. Mori, H. Takeshima, S. Narumiya, and S. Numa. 1989. Primary structure and functional expression of the cardiac dihydropyridine-sensitive calcium channel. *Nature*. 340:230–233.
- Mishina, M., T. Kurosaki, T. Tobimatsu, Y. Morimoto, M. Noda, T. Yamamoto, M. Terao, J. Lindstrom, T. Takahashi, M. Kuno, and S. Numa. 1984. Expression of functional acetylcholine receptor from cloned cDNAs. *Nature*. 307:604–608.
- Murphy, T. H., P. F. Worley, and J. M. Baraban. 1991. L-type voltage-sensitive calcium channels mediate synaptic activation of immediate early genes. *Neuron*. 7:625–635.

- Näbauer, M., G. Callewaert, L. Cleemann, and M. Morad. 1989. Regulation of calcium release is gated by calcium current, not gating charge, in cardiac myocytes. *Science*. 244:800–803.
- Okayama, H., and P. Berg. 1983. A cDNA cloning vector that permits expression of cDNA inserts in mammalian cells. *Mol. Cell. Biol.* 3:280–289.
- Page, K. M., C. Cantí, G. J. Stephens, N. S. Berrow, and A. C. Dolphin. 1998. Identification of the amino terminus of neuronal Ca^{2+} channel α_1 subunits α_{1B} and α_{1E} as an essential determinant of G-protein modulation. *J. Neurosci.* 18:4815–4824.
- Pemberton, K. E., and S. V. P. Jones. 1997. Inhibition of the L-type calcium channel by the five muscarinic receptors (m1–m5) expressed in NIH 3T3 cells. *Pflügers Arch.* 433:505–514.
- Pennartz, C. M. A., M. T. G. de Jeu, N. P. A. Bos, J. Schaap, and A. M. S. Geurtsen. 2002. Diurnal modulation of pacemaker potentials and calcium current in the mammalian circadian clock. *Nature*. 416:286–290.
- Platzter, J., J. Engel, A. Schrott-Fisher, K. Stephan, S. Bova, H. Chen, H. Zheng, and J. Striessnig. 2000. Congenital deafness and sinoatrial node dysfunction in mice lacking class D L-type Ca^{2+} channels. *Cell*. 102: 89–97.
- Rouse, S. T., S. E. Hamilton, L. T. Potter, N. M. Nathanson, and P. J. Conn. 2000. Muscarinic-induced modulation of potassium conductances is unchanged in mouse hippocampal pyramidal cells that lack functional M1 receptors. *Neurosci. Lett.* 278:61–64.
- Scheschonka, A., C. W. Dessauer, S. Sinnarajah, P. Chidiac, C.-S. Shi, and J. H. Kerhl. 2000. RGS3 is GTPase-activating protein for $G_{i\alpha}$ and $G_{q\alpha}$ and potent inhibitor of signalling by GTPase-deficient forms of $G_{q\alpha}$ and $G_{11\alpha}$. *Mol. Pharmacol.* 58:719–728.
- Seino, S., L. Chen, M. Seino, O. Blondel, J. Takeda, J. H. Johnson, and G. I. Bell. 1992. Cloning of the α_1 subunit of a voltage-dependent calcium channel expressed in pancreatic β cells. *Proc. Natl. Acad. Sci. USA*. 89:584–588.
- Shapiro, M., M. D. Loose, S. E. Hamilton, N. M. Nathanson, J. Gomeza, J. Wess, and B. Hille. 1999. Assignment of muscarinic receptor subtypes mediating G-protein modulation of Ca^{2+} channels by using knockout mice. *Proc. Natl. Acad. Sci. USA*. 96:10899–10904.
- Shapiro, M. S., J. P. Roche, E. J. Kaftan, H. Cruzblanca, K. Mackie, and B. Hille. 2000. Reconstitution of muscarinic modulation of the KCNQ2/KCNQ3 K^+ channels that underlie the neuronal M current. *J. Neurosci.* 20:1710–1721.
- Shenker, A., P. Goldsmith, C. G. Unson, and A. M. Spiegel. 1991. The G protein coupled to the thromboxane A_2 receptor in human platelets is a member of the novel G_q family. *J. Biol. Chem.* 266:9309–9313.
- Shistik, E., T. Ivanina, Y. Blumenstein, and N. Dascal. 1998. Crucial role of N terminus in function of cardiac L-type Ca^{2+} channel and its modulation by protein kinase C. *J. Biol. Chem.* 273:17901–17909.
- Smrcka, A. V., J. R. Hepler, K. O. Brown, and P. C. Sternweis. 1991. Regulation of polyphosphoinositide-specific phospholipase C activity by purified G_q . *Science*. 251:804–807.
- Snutch, T. P., W. J. Tomlinson, J. P. Leonard, and M. M. Gilbert. 1991. Distinct calcium channels are generated by alternative splicing and are differentially expressed in the mammalian CNS. *Neuron*. 7:45–57.
- Stewart, A. E., Z. Yan, D. J. Surmeier, and R. C. Foehring. 1999. Muscarine modulates Ca^{2+} channel currents in rat sensorimotor pyramidal cells via two distinct pathways. *J. Neurophysiol.* 81:72–84.
- Wei, J., E. A. Walton, A. Milici, and J. J. Buccafusco. 1994. m1–m5 muscarinic receptor distribution in rat CNS by RT-PCR and HPLC. *J. Neurochem.* 63:815–821.
- Weisskopf, M. G., E. P. Bauer, and J. E. Ledoux. 1999. L-type voltage-gated calcium channels mediate NMDA-independent associative long-term potentiation at thalamic input synapses to the amygdala. *J. Neurosci.* 19:10512–10519.
- Williams, M. E., D. H. Feldman, A. F. McCue, R. Brenner, G. Velicelebi, S. B. Ellis, and M. M. Harpold. 1992. Structure and functional expression of α_1 , α_2 , and β subunits of a novel human neuronal calcium channel subtype. *Neuron*. 8:71–84.
- Xu, W., and D. Lipscombe. 2001. Neuronal $\text{Ca}_v1.3\alpha_1$ L-type channels activate at relatively hyperpolarized membrane potentials and are incompletely inhibited by dihydropyridines. *J. Neurosci.* 21:5944–5951.